Journal of Sound and Vibration (2001) **240**(1), 117–129
doi:10.1006/jsvi.2000.3187, available online at http://www.idealibrary.com on IDEAL®

PARAMETRIC INSTABILITY OF DOUBLY CURVED PANELS SUBJECTED TO NON-UNIFORM HARMONIC LOADING

S. K. Sahu and P. K. Datta

Department of Aerospace Engineering, Indian Institute of Technology, (I.I.T.), Kharagpur 721302, *India.*
E-mail: pkdatta@aero.iitkgp.ernet.in

(*Received* 5 *April* 2000, *and in final form* 5 *July* 2000)

The parametric instability characteristics of doubly curved panels subjected to various in-plane static and periodic compressive edge loadings, including partial and concentrated edge loadings are studied using finite element analysis. The first order shear deformation theory is used to model the doubly curved panels, considering the effects of transverse shear deformation and rotary inertia. The theory used is the extension of dynamic, shear deformable theory according to the Sander's first approximation for doubly curved shells, which can be reduced to Love's and Donnell's theories by means of tracers. The effects of static load factor, aspect ratio, radius-to-thickness ratio, shallowness ratio, boundary conditions and the load parameters on the principal instability regions of doubly curved panels are studied in detail using Bolotin's method. Quantitative results are presented to show the effects of shell geometry and load parameters on the stability boundaries. Results for plates and cylindrical shells are also presented as special cases and are compared with those available in the literature.

1. INTRODUCTION

Structural elements subjected to in-plane periodic forces may lead to parametric resonance, due to certain combinations of the values of load parameters. The instability may occur below the critical load of the structure under compressive loads over a range or ranges of excitation frequencies. Several means of combating resonance such as damping and vibration isolation may be inadequate and sometimes dangerous with reverse results [1]. Thus, the parametric resonance characteristics are of great technical importance for understanding the dynamic systems under periodic loads. The parametric instability characteristics of plates subjected to uniform loads were studied by Hutt and Salam [2] using finite element method. Parametric resonance in shell structures under periodic loads had been of considerable interest since the subject was studied by Bolotin [3], Yao [4], Bieniek *et al.* [5] and Vijayaraghavan and Evan-Iwanowski [6]. The method of solution of these class of problems were to first reduce the equations of motion to a system of Mathieu–Hill equations and the parametric resonance characteristics were studied by different methods. A detailed study of resonances had carried out by Koval [7] using Donnel's shell theory. The stability of the steady state response of simply supported circular cylinders subjected to harmonic excitation was investigated by Radwin and Genin [8] using variational equations. The parametric instability characteristics of circular cylindrical shells under static and periodic loading were studied by Nagai and Yamaki [9] using Galerkin procedure and Hsu's method. The dynamic stability and non-linear parametric vibration of

0022-460X/01/060117 + 13 $35.00/0

isotropic cylindrical shells with added mass were considered by Kovtunov [10]. The dynamic instability of composite simply supported circular cylindrical shell was analysed by the method of multiple scale (MMS) by Cederbaum [11]. A perturbation technique was employed by Argento and Scott [12] to study the instability regions subjected to axial loading. The effects of static load and static snap through buckling on the instability for spherical and conical shells were investigated [13] using Galerkin method. The dynamic instability of conical shells were studied by Tani [14] using finite difference method and by Ng *et al.* [15] using generalized differential quadrature method. The parametric resonance of a rotating cylindrical shell subjected to periodic axial loads was investigated by Ng *et al.* [16]. The parametric resonance of cylindrical shells under combined static and periodic loading was studied using different thin shell theories by Lam and Ng [17, 18]. Most of the investigators studied the dynamic stability of uniformly loaded closed cylindrical shells with a simply supported boundary condition, using analytical approach.

The practical importance of stability analysis of doubly curved panels/open shells has been increased in structural, aerospace (skin panels in wings, fuselage, etc.), submarine hulls and mechanical applications but this type of open shells/panels have received less attention because of complexities involved. The free vibration of doubly curved shallow shells/curved panels was studied by a number of researchers [19–22] and well reviewed [23, 24]. Recently, the vibration under uniform initial stress and buckling stresses were studied for thick simply supported doubly curved open shells/panels through Hamilton's principle [25]. The buckling characteristics of isotropic flat panel [26, 27] and closed cylindrical shell [28, 29] due to concentrated loadings were also investigated. The study of the parametric instability behaviour of curved panels is new. Recently, the dynamic stability of uniformly loaded cylindrical panels with transverse shear effects is studied by Ng *et al.* [30]. Besides this, the applied load is seldom uniform and the boundary condition may be completely arbitrary in practice. The application of non-uniform loading and general boundary conditions on the structural component will alter the global quantities such as free vibration frequency, buckling load and dynamic instability region (DIR).

In the present study, the parametric instability of doubly curved panels subjected to various in-plane uniform and non-uniform, including partial and concentrated edge loadings are investigated. The influences of various parameters like effects of static and dynamic load factors, aspect ratio, radius-to-side ratio, thickness, various boundary conditions, percentage of loaded length and position of concentrated loads on the instability behaviour of curved panels have been examined. The present formulation of the problem is made general to accommodate a doubly curved panel with finite curvatures in both the directions having arbitrary load and boundary conditions.

2. THEORY AND FORMULATIONS

The basic configuration of the problem considered here is a doubly curved panel as shown in Figure 1, subjected to various non-uniform harmonic in-plane edge loadings.

2.1. GOVERNING EQUATIONS

The equation of equilibrium for free vibration of a shear deformable doubly curved panel subjected to in-plane external loading can be written as

$$\frac{\partial N_1}{\partial x} + \frac{\partial N_6}{\partial y} + \frac{1}{2} C_2 \left(\frac{1}{R_y} - \frac{1}{R_x} \right) \frac{\partial M_6}{\partial y} + C_1 \frac{Q_1}{R_x} = \rho h \frac{\partial^2 u}{\partial t^2} + \frac{\rho h^3}{12 R_y} \frac{\partial^2 \theta_x}{\partial t^2}, \tag{1}$$

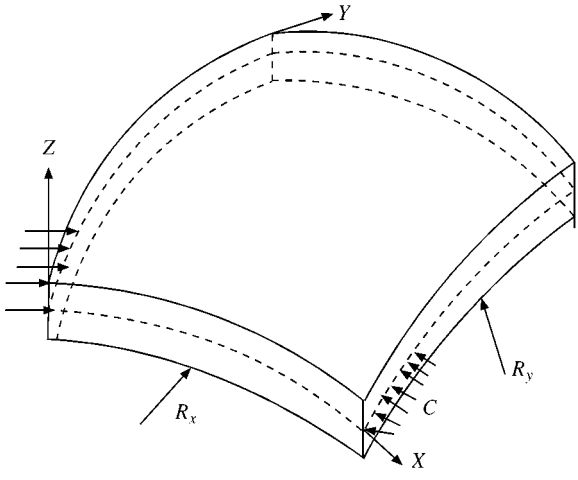

Figure 1. Geometry and co-ordinate systems of a doubly curved panel.

$$\frac{\partial N_6}{\partial x} + \frac{\partial N_2}{\partial y} - \frac{1}{2}C_2\left(\frac{1}{R_y} - \frac{1}{R_x}\right)\frac{\partial M_6}{\partial x} + C_1\frac{Q_2}{R_y} = \rho h\frac{\partial^2 v}{\partial t^2} + \frac{\rho h^3}{12R_y}\frac{\partial^2 \theta_y}{\partial t^2},$$

$$\frac{\partial Q_1}{\partial x} + \frac{\partial Q_2}{\partial y} - \frac{N_1}{R_x} - \frac{N_2}{R_y} + N_1^0\frac{\partial^2 w}{\partial x^2} + N_2^0\frac{\partial^2 w}{\partial x^2} = \rho h\frac{\partial^2 w}{\partial t^2},$$

$$\frac{\partial M_1}{\partial x} + \frac{\partial M_6}{\partial y} - Q_1 = \frac{\rho h^3}{12}\frac{\partial^2 \theta_x}{\partial t^2} + \frac{\rho h^3}{12R_y}\frac{\partial^2 u}{\partial t^2},$$

$$\frac{\partial M_6}{\partial x} + \frac{\partial M_2}{\partial y} - Q_2 = \frac{\rho h^3}{12}\frac{\partial^2 \theta_y}{\partial t^2} + \frac{\rho h^3}{12R_y}\frac{\partial^2 u}{\partial t^2},$$

where N_1^0 and N_2^0 are the external loading in X and Y directions respectively. C_1 and C_2 are tracers by which the analysis can be reduced to that of Sander's, Love's and Donnell's theories. The equation of motion can be written in matrix form as

$$[M]\{\ddot{q}\} + [[K_e] - P[K_g]]\{q\} = 0. \tag{2}$$

The in-plane load $P(t)$ is periodic and can be expressed in the form

$$P(t) = P_s + P_t \cos \Omega t, \tag{3}$$

where P_s is the static portion of P. P_t is the amplitude of the dynamic portion of P and Ω is the frequency of excitation. The static buckling load of elastic shell P_{cr} is the measure of the magnitudes of P_s and P_t,

$$P_s = \alpha P_{cr}, \qquad P_t = \beta P_{cr} \tag{4}$$

where α and β are termed as static and dynamic load factors respectively. Using equation (3), the equation of motion is obtained as

$$[M]\{\ddot{q}\} + [[K_e] - \alpha P_{cr}[K_g] - \beta P_{cr}[K_g]\cos \Omega t]\{q\} = 0. \tag{5}$$

Equation (5) represents a system of second order differential equations with periodic coefficients of the Mathieu–Hill type. The development of regions of instability arises from Floquet's theory which establishes the existence of periodic solutions. The boundaries of the dynamic instability regions are formed by the periodic solutions of period T and $2T$, where $T = 2\pi/\Omega$. The boundaries of the primary instability regions with period $2T$ are of practical importance [3] and the solution can be achieved in the form of the trigonometric series

$$q(t) = \sum_{k=1,3,5}^{\infty} \left[\{a_k\} \sin \frac{k\theta t}{2} + \{b_k\} \cos \frac{k\theta t}{2} \right]. \tag{6}$$

Substituting into equation (5) and if only the first term of the series is considered, equating coefficients of $\sin \theta t/2$ and $\cos \theta t/2$ the equation becomes

$$\left[[K_e] - \alpha P_{cr} [K_g] \pm \frac{1}{2} \beta P_{cr} [K_g] - \frac{\Omega^2}{4} [M] \right] \{q\} = 0. \tag{7}$$

Equation (7) represents an eigenvalue problem for known values of α,β and P_{cr}. The two conditions under a plus and minus sign correspond to two boundaries of the dynamic instability region. The eigenvalues are Ω, which give the boundary frequencies of the instability regions for given values of α and β. In this analysis, the computed static buckling load of the panel is considered as the reference load in line with Moorthy *et al.* [31] and Ganapathi *et al.* [32].

An eight-noded curved isoparametric quadratic element is employed in the present analysis with five degrees of freedom u, v, w, θ_x and θ_y per node. First order shear deformation theory (FSDT) is used and the shear correction coefficient has been employed to account for the non-linear distribution of the shear strains through the thickness. The displacement field assumes that mid-plane normal remains straight but not necessarily normal after deformation, so that

$$\begin{aligned} \bar{u}(x, y, z) &= u(x, y) + z\theta_x(x, y), \\ \bar{v}(x, y, z) &= v(x, y) + z\theta_y(x, y), \\ \bar{w}(x, y, z) &= w(x, y), \end{aligned} \tag{8}$$

where θ_x, θ_y are the rotations of the mid-surface.

Also, $\bar{u}$, $\bar{v}$, $\bar{w}$ and u, v, w are the displacement components in the x, y, z directions at any section and at mid-surface respectively. The constitutive relationships for the shell are given by

$$F = [D]\{\varepsilon\}, \tag{9}$$

where

$$F = [N_1, N_2, N_6, M_1, M_2, M_6, Q_1, Q_2]^{\mathrm{T}}, \tag{10}$$

$$[D] = \begin{bmatrix} \frac{Eh}{1-\nu^2} & \frac{\nu Eh}{1-\nu^2} & 0 & 0 & 0 & 0 & 0 & 0 \\ \frac{\nu Eh}{1-\nu^2} & \frac{Eh}{1-\nu^2} & 0 & 0 & 0 & 0 & 0 & 0 \\ 0 & 0 & \frac{Eh}{2(1+\nu)} & 0 & 0 & 0 & 0 & 0 \\ 0 & 0 & 0 & \frac{Eh^3}{12(1-\nu^2)} & \frac{\nu Eh^3}{12(1-\nu^2)} & 0 & 0 & 0 \\ 0 & 0 & 0 & \frac{Eh^3\nu}{12(1-\nu^2)} & \frac{Eh^3}{12(1-\nu^2)} & 0 & 0 & 0 \\ 0 & 0 & 0 & 0 & 0 & \frac{Eh^3}{24(1+\nu)} & 0 & 0 \\ 0 & 0 & 0 & 0 & 0 & 0 & \frac{Eh}{2{\cdot}4(1+\nu)} & 0 \\ 0 & 0 & 0 & 0 & 0 & 0 & 0 & \frac{Eh}{2{\cdot}4(1+\nu)} \end{bmatrix}. \tag{11}$$

A Reissner's shear correction factor of 5/6 is included for all numerical computations. Extension of shear deformable Sander's kinematic relations for doubly curved shells [33, 34] are used in the analysis. The linear strain–displacement relations are

$$\begin{aligned} \varepsilon_{xl} &= \frac{\partial u}{\partial x} + \frac{w}{R_x} + z\kappa_x, \\ \varepsilon_{yl} &= \frac{\partial v}{\partial y} + \frac{w}{R_y} + z\kappa_y, \\ \gamma_{xyl} &= \frac{\partial u}{\partial y} + \frac{\partial v}{\partial x} + z\kappa_{xy}, \\ \gamma_{yz} &= \frac{\partial w}{\partial y} + \theta_y - C_1\frac{v}{R_y}, \\ \gamma_{xz} &= \frac{\partial w}{\partial x} + \theta_x - C_1\frac{u}{R_x}, \end{aligned} \tag{12}$$

where

$$\kappa_x = \frac{\partial \theta_x}{\partial x}, \qquad \kappa_y = \frac{\partial \theta_y}{\partial y},$$

$$\kappa_{xy} = \frac{\partial \theta_x}{\partial y} + \frac{\partial \theta_y}{\partial x} + \frac{1}{2}C_2\left(\frac{1}{R_y} - \frac{1}{R_x}\right)\left(\frac{\partial v}{\partial x} - \frac{\partial u}{\partial y}\right). \tag{13}$$

The element geometric stiffness matrix for the doubly curved panel is derived using the non-linear strain components as

$$\varepsilon_{xnl} = \frac{1}{2}\left(\frac{\partial u}{\partial x} + \frac{w}{R_x}\right)^2 + \frac{1}{2}\left(\frac{\partial v}{\partial x}\right)^2 + \frac{1}{2}\left(\frac{\partial w}{\partial x} - \frac{u}{R_x}\right)^2 + \frac{1}{2}z^2\left[\left(\frac{\partial \theta_x}{\partial x}\right)^2 + \left(\frac{\partial \theta_y}{\partial x}\right)^2\right],$$

$$\varepsilon_{ynl} = \frac{1}{2}\left(\frac{\partial u}{\partial y}\right)^2 + \frac{1}{2}\left(\frac{\partial v}{\partial y} + \frac{w}{R_y}\right)^2 + \frac{1}{2}\left(\frac{\partial w}{\partial y} - \frac{v}{R_y}\right)^2 + \frac{1}{2}z^2\left[\left(\frac{\partial \theta_x}{\partial y}\right)^2 + \left(\frac{\partial \theta_y}{\partial y}\right)^2\right],$$

$$\gamma_{xynl} = \left[\left(\frac{\partial u}{\partial x} + \frac{w}{R_x}\right)\frac{\partial u}{\partial y} + \frac{\partial v}{\partial x}\left(\frac{\partial v}{\partial y} + \frac{w}{R_y}\right) + \left(\frac{\partial w}{\partial x} - \frac{u}{R_x}\right)\left(\frac{\partial w}{\partial y} - \frac{v}{R_y}\right)\right],$$

$$+ z^2\left[\left(\frac{\partial \theta_x}{\partial x}\right)\left(\frac{\partial \theta_x}{\partial y}\right) + \left(\frac{\partial \theta_y}{\partial x}\right)\left(\frac{\partial \theta_y}{\partial y}\right)\right]. \tag{14}$$

The element matrices are derived as:

Elastic stiffness matrix:

$$[K_e]_e = \int [B]^{\mathrm{T}}[D][B]\,\mathrm{d}x\,\mathrm{d}y. \tag{15}$$

Geometric stiffness matrix:

$$[K_g]_e = \int [B_g]^{\mathrm{T}}[\bar{\sigma}][B_g]\,\mathrm{d}x\,\mathrm{d}y. \tag{16}$$

Consistent mass matrix:

$$[M]_e = \int [N]^{\mathrm{T}}[I][N]\,\mathrm{d}x\,\mathrm{d}y. \tag{17}$$

The overall matrices $[K_e]$, $[K_g]$ and $[M]$ are obtained by assembling the corresponding element matrices.

2.2. COMPUTER PROGRAM

A computer program has been developed to perform all the necessary computations. Element elastic stiffness matrices and mass matrices are obtained using a standard procedure. The geometric stiffness matrix is essentially a function of the in-plane stress distribution in the element due to applied edge loadings. Since the stress field is non-uniform, plane stress analysis is carried out using the finite element method to determine the stresses and these are used to formulate the geometric stiffness matrix. Reduced integration technique is adopted in order to avoid possible shear locking. Element matrices are assembled into global matrices, using skyline technique. Subspace iteration method is adopted throughout to solve the eigenvalue problems.

3. RESULTS AND DISCUSSIONS

The convergence studies have been carried out for fundamental frequencies of vibration of cantilevered doubly curved shells/panels for three different cases and the results are compared with Leissa *et al.* [20] in Table 1. From the above convergence study, 10×10 mesh has been employed to idealize the panel in the subsequent analysis. The idealization is chosen in order to apply compression to a small fraction of the edge length and also for

TABLE 1

Convergence of non-dimensional fundamental frequencies without in-plane load of doubly curved shells/panels ($a/b = 1$, $b/h = 100$, $b/R_y = 0{\cdot}2$, $v = 0{\cdot}3$. *Non-dimensional frequency*, $\omega = \bar{\omega}a^2\sqrt{(\rho h/D)}$)

Mesh division	Non-dimensional frequencies of shells		
	Cylindrical	Spherical	Hyperbolic paraboloid
4×4	8·3837	6·6529	6·6072
8×8	8·3679	6·5787	6·5015
10×10	8·3653	6·5748	6·4969
Leissa [20]	(8·3683)	(6·5854)	(6·5038)

TABLE 2

Non-dimensional fundamental frequencies and buckling loads for the doubly curved shell/panel ($a/b = 1$, $v = 0{\cdot}3$. *Non-dimensional frequency*, $\omega = \bar{\omega}h\sqrt{(\rho/G)}$, $\lambda = N_x b^2/D$)

			Non-dimensional frequencies		Non-dimensional bucklingloads	
a/h	a/R_x	b/R_y	Present FEM	Matsunaga [25]	Present FEM	Matsunaga [25]
10	0	0	0·09303	0·09315	36·8284	36·9242
	0·2	0·2	0·09822	0·09826	41·0487	41·0872
	0	0·2	0·09426	0·09436	37·8075	37·8904
	−0·2	0·2	0·09264	0·09276	36·5235	36·6162
20	0	0	0·02386	0·02387	38·7757	38·7945
	0·2	0·2	0·02873	0·02872	56·2143	56·1620
	0	0·2	0·02515	0·02515	43·0581	43·0670
	−0·2	0·2	0·02373	0·02378	38·4618	38·5033

convergence criterion. To validate the formulation further, the free vibration frequency and critical buckling load for simply supported uniformly loaded shells/panels, are compared with the literature [25] in Table 2. The above studies indicate good agreement between the present study and those from the literature. Once the free vibration and buckling results are validated, the dynamic instability studies are made.

3.1. PARAMETRIC INSTABILITY STUDIES

The parametric instability regions are plotted for a uniaxially loaded doubly curved panel with/without static component to consider the effects of static load factor, aspect ratio, boundary conditions, radius-to-thickness ratio, shallowness ratio, load bandwidth and positions of concentrated edge loading. A simply supported doubly curved panel of dimensions $a = b = 400$ mm, $h = 4$ mm, $E = 0{\cdot}7e11$ N/m^2, $v = 0{\cdot}3$, $\rho = 2800$ kg/m^3, $R_x = R_y = 2000$ mm is described as a standard case and the computed buckling load of this panel is taken as the reference load in line with Moorthy *et al.* [31]. The non-dimensional excitation frequency $\Omega = \bar{\Omega}a^2\sqrt{\rho h/D}$ is used throughout the dynamic instability studies (unless otherwise mentioned), where $\bar{\Omega}$ is the excitation frequency in rad/s,

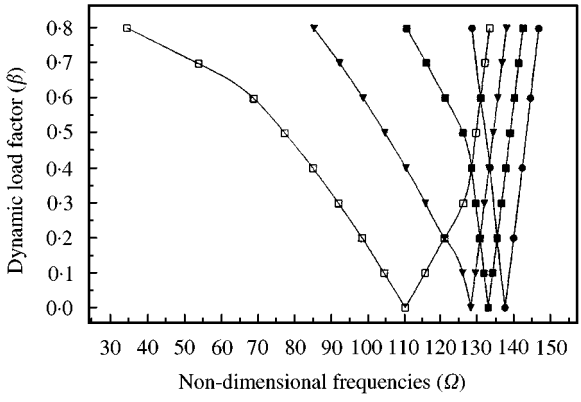

Figure 2. Effect of static load factor on instability region of a fully loaded curved panel: $a/b = 1$, $a/R_x = 0{\cdot}2$, $b/R_y = 0{\cdot}2$, for $\alpha = 0{\cdot}0, 0{\cdot}2, 0{\cdot}4, 0{\cdot}8$. Static load factor ($\alpha$): ● = 0, ■ = 0·2, ▼ = 0·4, □ = 0·6.

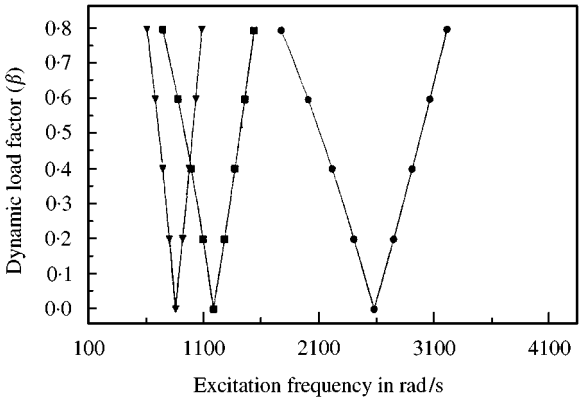

Figure 3. Effect of aspect ratio on instability region of the curved panel for $a/b = 1, 2$ and 3, $a/R_x = 0$, $b/R_y = 0{\cdot}2$, $\alpha = 0{\cdot}2$. Aspect ratio: ● = 1, ■ = 2, ▼ = 3.

$D = Eh^3/12(1 - \nu^2)$. The effect of static component of load for $\alpha = 0{\cdot}0, 0{\cdot}2, 0{\cdot}4$ and $0{\cdot}6$ on the instability regions is shown in Figure 2. Due to increase of static component, the instability regions tend to shift to lower frequencies and become wider. Figure 3 shows the effect of aspect ratio on instability regions. It is observed that the onset of dynamic stability occurs much later with decrease of the aspect ratio but with increasing width of instability regions. Figure 4 shows the influence of different boundaries (SSSS, SCSC, CCCC) on the principal instability regions. As expected, the instability occurs at a higher excitation frequency from simply supported to clamped edges due to the restraint at the edges. The width of the instability regions are also decreased with the increase of restraint at the edges. The effect of radius-to-thickness ratio on instability regions is shown in Figure 5. The onset of dynamic instability regions are observed to be increasing with decrease of R_y/h ratio. Figure 6 shows the effect of shallowness ratio on instability regions. As seen from the figure, the instability excitation frequency is higher for decrease of shallowness by decreasing R_x and R_y. Studies have also been made (Figure 7) for comparison of instability regions for different shell

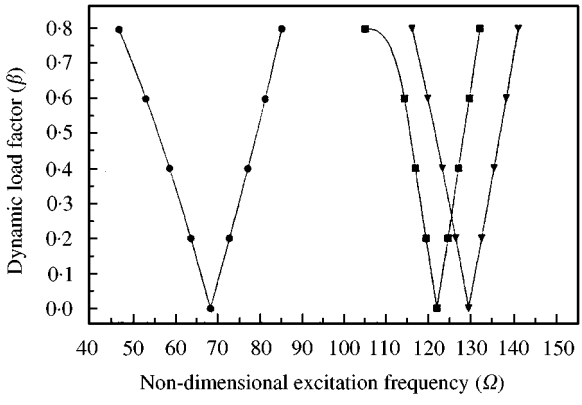

Figure 4. Effect of boundary conditions (SSSS, SCSC, CCCC) on instability region of the curved panel for $a/b = 1$, $a/R_x = 0{\cdot}0$, $b/R_y = 0{\cdot}2$ and $\alpha = 0{\cdot}2$. Boundary: ● = SSSS, ■ = SCSC, ▼ = CCCC.

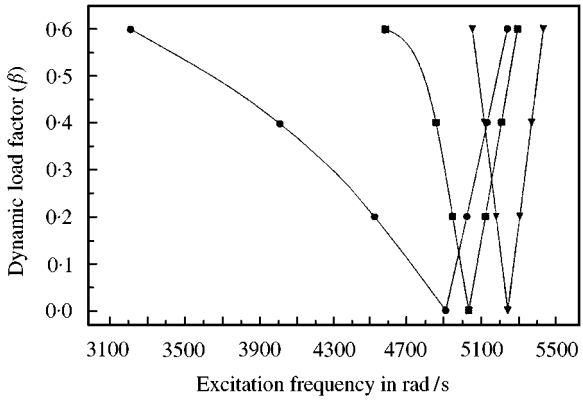

Figure 5. Effect of thickness on instability region of the curved panel for $a/b = 1$, $R_x/h = R_y/h = 625$, 500, 375 and $\alpha = 0{\cdot}2$. R/h ratio: ● = 625, ■ = 500, ▼ = 375.

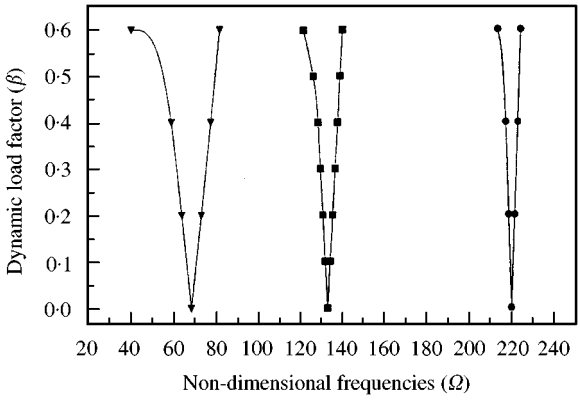

Figure 6. Effect of R_y/b on instability region of the curved panel for $a/b = 1$, $R_x/a = R_y/b = 3$, 5, 10, $\alpha = 0{\cdot}2$. Rx/a = Ry/b: ● = 3, ■ = 5, ▼ = 10.

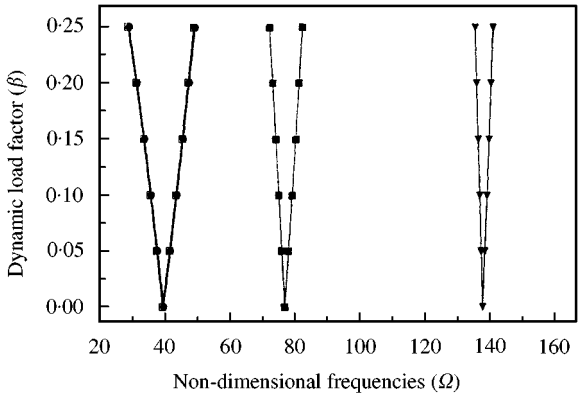

Figure 7. Effect of curvature on instability region of different curved panels for $a/b = 1$, flat panel ($a/R_x = b/R_y = 0$), cylindrical ($a/R_x = 0$, $b/R_y = 0{\cdot}2$), spherical ($a/R_x = b/R_y = 0{\cdot}2$), hyperbolic paraboloid ($a/R_x = -0{\cdot}2, b/R_y = 0{\cdot}2$) and $\alpha = 0{\cdot}0$. Curved panel: ● = plate, ■ = cylindrical, ▼ = spherical, □ = hyperbolic parabolid.

TABLE 3

Primary regions of instability for the doubly curved panel subjected to different loading conditions ($a = b = 400$ mm, $h = 4$ mm, $E = 0{\cdot}7e11$ N/m^2, $\nu = 0{\cdot}3$, $\rho = 2800$ kg/m^3, $R_x = R_y = 2000$ mm, $\alpha = 0{\cdot}2$. *Non-dimensional frequency*, $\Omega = \bar{\Omega}a^2\sqrt{\rho h/D}$)

	Uniaxial loading		Biaxial loading	
β	U	L	U	L
0	133·0780	133·0780	128·3204	128·3204
0·2	135·3942	130·7208	133·0780	123·3793
0·4	137·6714	128·3203	137·6714	118·2320
0·6	139·9115	121·0582	142·1164	107·3603
0·8	142·1164	110·2660	146·4265	91·6730

geometries. It is observed that the excitation frequency increases with introduction of curvatures from plate to doubly curved panel. However, the hyperbolic paraboloid shows similar instability behaviour as that of a flat panel with no stiffness being added due to the curvature of the panel. Similar observations were also obtained by Leissa and Kadi [19] on a study of vibration of shells. The study is then extended for biaxial loading on the parametric excitation behaviour of doubly curved panels. The results are presented in Table 3. It was observed that instability appears at lower excitation frequency with increasing dynamic instability region. The investigation is then extended for partial and concentrated edge loading from one end. The load parameter of $c/b = 0$ corresponds to concentrated loads at the two opposite edges. A double pair of partial and concentrated loading from both ends and other types of non-uniform loading are also studied. The curved panels under non-uniform loading behave differently to that of under uniform loading. The onset of dynamic stability occurs earlier with the increase of percentage of loaded edge length. Figure 8 shows that the instability occurs later for a small patch loading ($c/b = 0{\cdot}2$) as compared to a higher bandwidth ($c/b = 0{\cdot}8$). This may be due to the constraint at the edges. Similarly, the instability also depends on the positions of concentrated loading

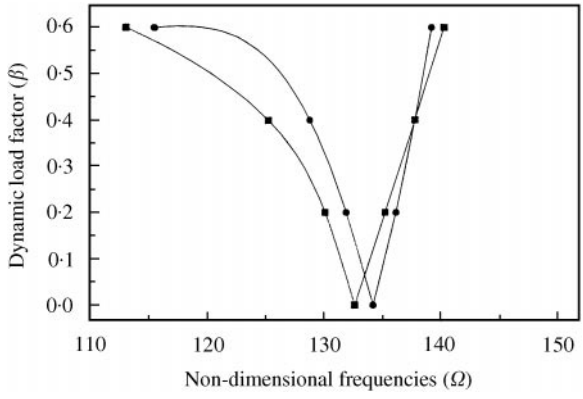

Figure 8. Effect of percentage of loaded edge length on instability region of a spherical panel for $a/b = 1$, $a/R_x = b/R_y = 0{\cdot}2$, $c/b = 0{\cdot}2$ and $0{\cdot}8$, $\alpha = 0{\cdot}2$. z of loading (c/b): ● $= 0{\cdot}2$, ■ $= 0{\cdot}8$.

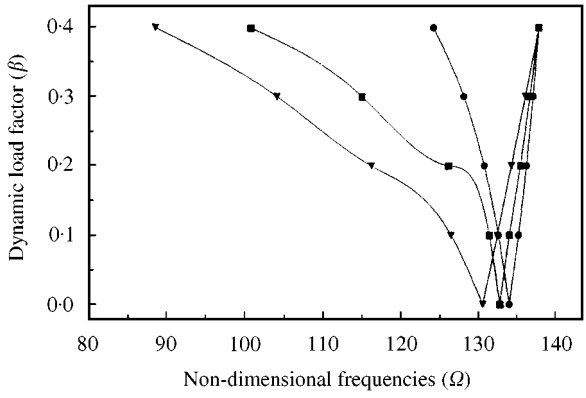

Figure 9. Effect of position of concentrated load on instability region of a spherical shell for $a/b = 1$, $a/R_x = b/R_y = 0{\cdot}2$, $c/b = 0$, $0{\cdot}25$ and $0{\cdot}5$, $\alpha = 0{\cdot}2$. Load position (c/b): ● $= 0$, ■ $= 0{\cdot}25$, ▼ $= 0{\cdot}5$.

(Figure 9). As observed, the instability occurs at lower excitation frequencies with increase of distance from the edges (c/b). The curved panel with a small patch of loading behaves in a similar manner to that of a panel subjected to a pair of concentrated loading near the edges and shows highest stiffness among all the loadings considered.

4. CONCLUSION

The results of the stability studies of the shells can be summarized as follows:

1. Due to static component, the instability regions tend to shift to lower frequencies with wide instability regions showing destabilizing effect on the dynamic stability behaviour of the curved panel.
2. The onset of instability occurs at higher excitation frequencies with lower R_y/h ratios.
3. The instability regions have been influenced due to restraint provided at the edges.
4. The onset of instability region appears earlier for rectangular panels with the increase in aspect ratio.

5. The instability regions start at higher frequencies with lower shallowness ratio.
6. The curved panels show more stiffness with addition of curvatures. But the hyperbolic paraboloid panels behave like a plate with no stiffness being added due to curvature of the shell.
7. The instability appears at lower excitation frequency with increasing dynamic instability region with biaxial loading.
8. The onset of instability occurs at higher excitation frequencies for small patch and concentrated loads near the edges but at lower frequencies for long bandwidth and concentrated loads away from the edges.

REFERENCES

1. R. M. Evan-Iwanowski 1965 *Applied Mechanics Review* **18**, 699–702. On the parametric response of structures.
2. J. M. Hutt and A. E. Salam 1971 *ASCE Journal of Engineering Mechanics* **3**, 879–899. Dynamic instability of plates by finite element.
3. V. V. Bolotin 1964 *The Dynamic Stability of Elastic Systems*. San Francisco: Holden-Day.
4. J. C. Yao 1965 *Journal of Applied Mechanics* **32**, 109–115. Nonlinear elastic buckling and parametric excitation of a cylinder under axial loads.
5. M. P. Bieniek, T. C. Fan and L. M. Lackman 1966 *AIAA Journal* **4**, 495–500. Dynamic stability of cylindrical shells.
6. A. Vijayraghavan and Evanwanowski 1967 *ASME Journal Applied Mechanics* **31**, 985–990. Parametric instability of circular cylindrical shells.
7. L. R. Koval 1974 *Journal of Acoustical Society of America* **55**, 91–97. Effect of longitudinal resonance on the parametric stability of an axially excited cylindrical shells.
8. H. R. Radwan and J. Genin 1978 *Journal of Sound and Vibration* **56**, 373–382. Dynamic instability in cylindrical shells.
9. K. Nagai and N. Yamaki 1978 *Journal of Sound and Vibration* **58**, 425–441. Dynamic stability of circular cylindrical shells under periodic compressive forces.
10. V. B. Kovtunov 1993 *Computers and Structures* **46**, 149–156. Dynamic stability and nonlinear parametric vibration of cylindrical shells.
11. G. Cederbaum 1992 *International Journal Mechanical Sciences* **34**, 241–250. Analysis of parametrically excited laminated shells.
12. A. Argento and R. A. Scott 1993 *Journal of Sound and Vibration* **162**, 323–332. Dynamic instability of layered anisotropic circular cylindrical shells, part II: numerical results.
13. Z. M. Ye 1997 *Journal of Sound and Vibration* **202**, 303–311. The non-linear vibration and dynamic instability of thin shallow shells.doi:10.1006/jsvi.1996.0827.
14. J. Tani 1976 *ASME Journal of Applied Mechanics* **43**, 87–91. Influence of deformations prior to instability on the dynamic instability of conical shells under periodic axial load.
15. T. Y. Ng, Li Hua, K. Y. Lam and C. T. Loy 1999 *International Journal for Numerical Methods in Engineering* **44**, 819–837. Parametric instability of conical shells by the generalized differential quadrature method.
16. T. Y. Ng, K. Y. Lam and J. N. Reddy 1998 *Journal of Sound and Vibration* **214**, 513–529. Parametric resonance of a rotating cylindrical shell subjected to periodic axial load.doi.10.1006/jsvi.1998.1550.
17. K. Y. Lam and T. Y. Ng 1997 *Journal of Sound and Vibration* **207**, 497–520. Dynamic stability of cylindrical shells subjected to conservative periodic axial loads using different shell theories.doi.10.1006/jsvi.1997.1186.
18. K. Y. Lam and T. Y. Ng 1999 *AIAA Journal* **37**, 137–140. Parametric resonance of cylindrical shells by different shell theories.
19. A. W. Leissa and A. S. Kadi 1971 *Journal of Sound and Vibration* **16**, 173–187. Curvature effects on shallow shell vibration.
20. A. W. Leissa, J. K. Lee and A. J. Wang 1983 *International Journal of Solids Structures* **19**, 411–424. Vibrations of cantilevered doubly curved shallow shells.
21. T. Aksu 1997 *Computers and Structures* **65**, 687–694. A finite element formulation for free vibration analysis of shells of general shape.

22. A. BHIMARADDI 1991 *International Journal of Solids and Structures* **27**, 897–913. Free vibration analysis of doubly curved shallow shells on rectangular planform using three-dimensional elasticity theory.
23. M. S. QATU 1992 *Shock and Vibration Digest* **24**, 3–15. Review of shallow shell vibration research.
24. K. M. LIEW, C. W. LIM and S. KITIPORNCHAI 1997 *Applied Mechanics Review* **50**, 431–444. Vibration of shallow shells: a review with bibliography.
25. H. MATSUNAGA 1999 *Journal of Sound and Vibration* **225**, 41–60. Vibration and stability of thick simply supported shallow shells subjected to in-plane stresses.doi: 10.1006/jsvi.1999.2234.
26. A. W. LEISSA and E. F. AYUB 1988 *Journal of Sound and Vibration* **127**, 155–171. Vibration and buckling of simply supported rectangular plate subjected to a pair of in-plane concentrated forces.
27. A. W. LEISSA and E. F. AYUB 1989 *Journal of Engineering Mechanics, ASCE* **115**, 2749–2762. Tension buckling of Rectangular sheets due to concentrated forces.
28. A. LIBAI and D. DURBAN 1977 *Journal of Applied Mechanics* **44**, 714–720. Buckling of cylindrical shells subjected to non-uniform axial loads.
29. D. DURBAN and E. ORE 1999 *ASME Journal of Applied Mechanics* **66**, 374–379. Plastic buckling of circular cylindrical shells under non-uniform axial loads.
30. T. Y. NG, K. Y. LAM and J. N. REDDY 1999 *International Journal of Solids and Structures* **36**, 3483–3496. Dynamic stability of cylindrical panels with transverse shear effects.
31. J. MOORTHY, J. N. REDDY and R. H. PLAUT 1990 *International Journals of Solids Structures* **26**, 801–811. Parametric instability of laminated composite plates with transverse shear deformation.
32. M. GANAPATHI, P. BOISSE and D. SOLAUT 1999 *International Journal for Numerical Methods in Engineering* **46**, 943–956. Non-linear dynamic stability analysis of composite laminates under periodic in-plane loads.
33. J. N. REDDY 1984 *Journal of Engineering Mechanics, ASCE* **110**, 794–809. Exact solutions of moderately thick laminated shells.
34. K. CHANDRASHEKHARA 1989 *Computers and Structures* **33**, 435–440. Free vibrations of anisotropic laminated doubly curved shells.

APPENDIX A: NOMENCLATURE

a, b	dimensions of shell
R_x, R_y	radii of curvatures
c	percentage of loaded length/distance of concentrated load from edge
E	Young's modulus
v	Poisson's ratio
ρ	mass density
G	shear modulus
$[K]$	stiffness matrix
$[K_g]$	geometric stiffness matrix
$[M]$	mass matrix
$\{q\}$	vector of generalized co-ordinates
w	deflection of mid-plane of shell
θ_x, θ_y	rotations about axes
Ω, ω	frequency of forcing function and transverse vibration
α, β	static and dynamic load factors
P_{cr}	critical buckling load